

# Application of Optimal Catalyst Activity Distribution Theory

Hua Wu

Ausimont Research and Development Center, Montedison, 20021 Bollate, Milano, Italy

Following the initial finding of Morbidelli et al. (1982) that the optimal catalyst activity distribution (OCAD) in a pellet is given by a Dirac delta function for single reacting systems, such activity distributions have received great attention. The work in this area has been reviewed by Dougherty and Verykios (1987) and recently by Gavrilidis et al. (1993). Now, it can be generally concluded that for any catalyst performance index, for example, effectiveness, selectivity, or yield, and for the most general case of an arbitrary number of reactions, following arbitrary kinetics occurring in a nonisothermal pellet with finite external heat-and-mass-transfer resistance, the OCAD is a Dirac delta function.

The application of the OCAD theory to maximize the outlet conversion of a fixed-bed catalytic reactor has been described by Morbidelli et al. (1986a) for single isothermal reacting systems. It was shown that the rigorous optimal solution for the maximum outlet conversion is obtained by maximizing the local conversion along the reactor axis. In other words, the optimization problem of the reactor is determined strictly by the local optimization of each pellet.

In the present work, the application of the OCAD theory to maximize the outlet yield or selectivity of a fixed-bed catalytic reactor is discussed for isothermal parallel reacting systems. It is interesting to find that, unlike the case for the maximum outlet conversion, the local optimization of each pellet does not necessarily give rise to the maximum outlet yield or selectivity. Instead, if the OCAD in pellets is considered globally as a parameter to be optimized with respect to the reactor outlet performance, a higher outlet yield or selectivity can be obtained in some specific situations.

## Basic Equations

Consider the following isothermal parallel reacting system:



Each of the reactions follows a general Langmuir-Hinshelwood kinetic law:

$$r_1 = k_1 f_1(C_A) = \frac{k_1 C_A^{m_1}}{(1 + K_A C_A)^{\alpha_1}} \quad (1)$$

$$r_2 = k_2 f_2(C_A) = \frac{k_2 C_A^{m_2}}{(1 + K_A C_A)^{\alpha_2}} \quad (2)$$

With the assumptions of ideal plug flow in the fluid phase and negligible interpellet mass-transfer resistance, and with the particular Dirac delta form of the catalyst activity distribution in pellets (Morbidelli et al., 1982):

$$a(s) = \frac{\delta(s - \bar{s})}{(n + 1)\bar{s}^n} \quad (3)$$

the following equations can be obtained from the steady-state mass balances both for the reactor and for the pellet:

$$\frac{dv_1}{dz} = -Da \cdot R_A = -Da \cdot [F_1(\bar{u}_1) + R^i F_2(\bar{u}_2)] \quad (4)$$

$$\frac{dv_2}{dz} = Da \cdot R_B = Da \cdot F_1(\bar{u}_1) \quad (5)$$

with initial conditions:

$$v_1 = 1; \quad v_2 = 0, \quad \text{at } z = 0 \quad (6)$$

where

$$F_1(\bar{u}_1) = f_1(\bar{C}_A) / f_1(C_{Af}) = \left( \frac{1 + \sigma}{1 + \sigma \cdot \bar{u}_1} \right)^{\alpha_1} \cdot \bar{u}_1^{m_1}; \quad (7)$$

$$F_2(\bar{u}_1) = f_2(\bar{C}_A) / f_2(C_{Af}) = \left( \frac{1 + \sigma}{1 + \sigma \cdot \bar{u}_1} \right)^{\alpha_2} \cdot \bar{u}_1^{m_2}; \quad (8)$$

and  $\bar{u}_1 = u_1(\bar{s})$ , which together with  $\bar{s}$  and  $v_1$  satisfies the following algebraic equation (Morbidelli et al., 1986b):

$$\frac{v_1 - \bar{u}_1}{\phi^2 R_A} = 1 - \bar{s} \quad \text{for } n=0, \quad (9a)$$

or

$$\frac{v_1 - \bar{u}_1}{\phi^2 R_A} = -\ln \sqrt{\bar{s}} \quad \text{for } n=1, \quad (9b)$$

or

$$\frac{v_1 - \bar{u}_1}{\phi^2 R_A} = \frac{1 - \bar{s}}{3\bar{s}} \quad \text{for } n=2 \quad (9c)$$

For the given parallel reacting system ( $I$ ), the yield ( $Y_c$ ) and the selectivity ( $S_c$ ) of the catalyst pellet with respect to the product B can be expressed respectively as (Wu et al., 1990):

$$Y_c = \frac{(n+1) \int_0^1 a(s) F_1(u_1) s^n ds}{1 + R^i} \quad (10)$$

$$S_c = \frac{\int_0^1 a(s) F_1(u_1) s^n ds}{\int_0^1 a(s) [F_1(u_1) + R^i F_2(u_1)] s^n ds} \quad (11)$$

which, when the Dirac delta type of catalyst activity distribution (Eq. 3) is considered, are reduced to

$$Y_c = \frac{F_1(\bar{u}_1)}{1 + R^i} \quad (12)$$

$$S_c = \frac{F_1(\bar{u}_1)}{F_1(\bar{u}_1) + R^i F_2(\bar{u}_1)} \quad (13)$$

The outlet yield ( $Y$ ) and the outlet selectivity ( $S$ ) of the reactor can be simply defined as:

$$Y = v_2^o \quad (14)$$

$$S = \frac{v_2^o}{1 - v_1^o} \quad (15)$$

When the optimization of the reactor is solved by considering the local optimization of each pellet, the problem is reduced to find the optimal active location in pellets at each  $z \in [0, 1]$ , which maximizes  $Y_c$  (or  $S_c$ ). The general procedure is first to find the optimal value of  $\bar{u}_1 \in (0, 1]$  from Eq. 12 and Eq. 13, which gives the maximum value of  $Y_c$  (or  $S_c$ ), and then to find the optimal active location ( $\bar{s}$ ) through Eq. 9. Note that when  $\bar{u}_1 \geq v_1$ , we have to let  $\bar{u}_1 = v_1$  and  $\bar{s} = 1$ , that is, the external surface is the optimal active location. This optimization approach is referred to as the *local OCAD approach*.

Another approach to be examined in this work is that instead of finding locally the optimal value of  $\bar{u}_1$  for the maximum  $Y_c$  (or  $S_c$ ), we find globally the optimal value of  $\bar{u}_1 \in (0, 1]$  which maximizes the outlet yield ( $Y$ ) or the outlet selectivity ( $S$ ).  $\bar{u}_1$  must be found numerically through the one-parameter estimation process. For any given value of  $\bar{u}_1$ , the procedure is actually the same as that in the local OCAD approach. Such an approach is referred to as the *global OCAD approach*.

In the next section, the two approaches are compared for some specific parallel reacting systems.

## Results and Discussion

### Maximum outlet yield

Let us consider the case:  $m_1 = m_2 = 1$ ,  $\alpha_1 = 2$  and  $\alpha_2 = 1$  in Eqs. 1 and 2. Equations 7 and 8 become:

$$F_1(\bar{u}_1) = (1 + \sigma)^2 \cdot \frac{\bar{u}_1}{(1 + \sigma \cdot \bar{u}_1)^2} \quad (16)$$

$$F_2(\bar{u}_1) = (1 + \sigma) \cdot \frac{\bar{u}_1}{1 + \sigma \cdot \bar{u}_1} \quad (17)$$

Now both the local and global OCAD approaches are applied to this parallel reacting system for the maximum outlet yield. The typical solution is shown respectively in Figure 1 (the local OCAD approach) and Figure 2 (the global OCAD approach), where  $\sigma = 20$ .

It is readily found from Eq. 12 that the maximum yield ( $Y_c$ ) of the catalyst pellet is attained at  $\bar{u}_1 = 1/\sigma$ . Then, the active catalyst should be located at the position in the pellet where  $\bar{u}_1 = 1/\sigma$ . It follows in Figure 1 that in the first portion of the reactor,  $z \in [0, \hat{z}]$  where  $v_1 > 1/\sigma = 0.05$ , we have that  $\bar{u}_1 = 0.05$  and  $\bar{s} < 1$ . At  $z = \hat{z}$ ,  $\bar{u}_1 = v_1 = 0.05$  and  $\bar{s} = 1$ , and then in the second portion,  $z \in (\hat{z}, 1]$ , since  $v_1 < 0.05$ ,  $\bar{u}_1 = v_1$  and  $\bar{s} = 1$ . The outlet yield ( $Y$ ) through the local OCAD approach is 0.914.

The solution with the global OCAD approach shown in Figure 2 indicates that for the maximum outlet yield the optimal value of  $\bar{u}_1$  is 0.02362 rather than 0.05. The obtained outlet yield is 0.934, higher than that with the local OCAD approach. By comparing Figure 2 with Figure 1, it is seen that since the

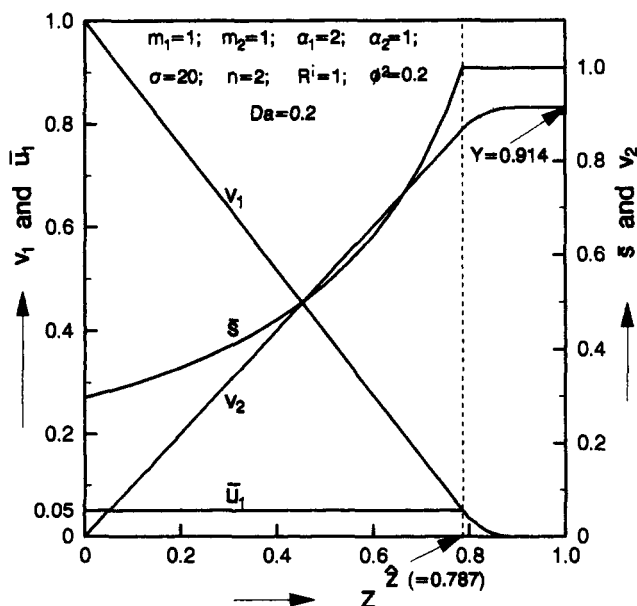
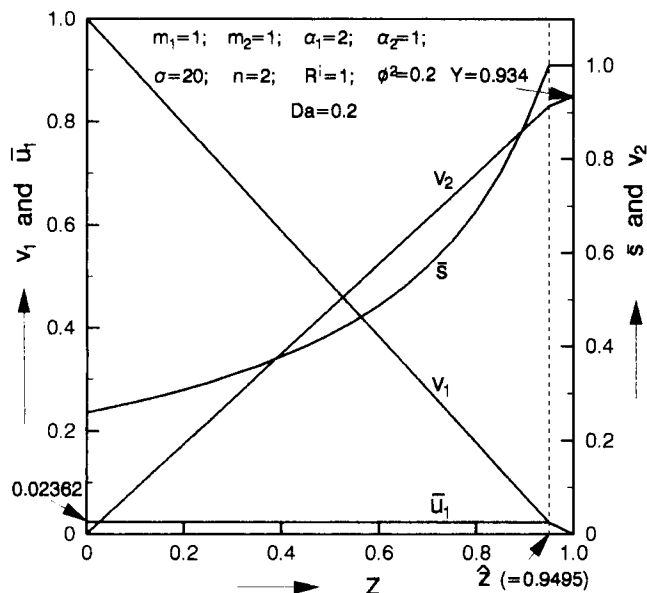


Figure 1. Optimal solution for the maximum outlet yield from local OCAD approach.

Profiles of the active location  $\bar{s}$ , the reactant concentration  $\bar{u}_1$  at  $s = \bar{s}$ , and  $v_1$  and  $v_2$  in the fluid phase along the reactor axis.



**Figure 2. Optimal solution for the maximum outlet yield from the global OCAD approach.**

Profiles of the active location  $\bar{s}$ , the reactant concentration  $\bar{u}_1$  at  $s=\bar{s}$ , and  $v_1$  and  $v_2$  in the fluid phase along the reactor axis.

value of  $\bar{u}_1$  is lower the value of  $\hat{z}$  is now greater, that is, the first portion of the reactor where  $\bar{s} < 1$  is longer.

The failure of the local OCAD approach in giving the maximum outlet yield can be easily explained once one notices that for the given reacting system (Eqs. 16 and 17), the selectivity of the catalyst pellet increases as  $\bar{u}_1$  decreases. The yield is practically the product of conversion and selectivity. To get the maximum outlet yield, one should weigh the conversion and the selectivity both locally and globally. In Figure 1 from the local point of view the conversion and the selectivity are weighed very well such that at each  $z \in [0, 1]$  the yield is maximized locally, but from the global point of view, the conversion is over-considered, because it is already 0.99998 at  $z=0.9$  leading to the remaining portion of the reactor ( $z \in [0.9, 1]$ ) being practically unused. In the case of Figure 2, since  $\bar{u}_1 = 0.02362 < 0.05$  in the first portion of the reactor, the selectivity becomes higher, that is, slightly over-considered. This leads to a lower local conversion and yield, but globally, since the whole reactor has been utilized, the outlet conversion is still very high (0.9994). As a result, the global OCAD solution gives a higher outlet yield, and it is therefore the optimal one.

In Figure 3, the optimal outlet yields and the values of  $\hat{z}$  obtained from the two approaches are shown as functions of Damköhler number ( $Da$ ), where the dashed lines denote the results from the local OCAD approach. It is clear that the difference between the two approaches exists only when  $\hat{z} < 1$ , that is, when the reactor has two distinct portions: the first portion,  $z \in [0, \hat{z}]$ , where  $\bar{s} < 1$ , and the second portion,  $z \in [\hat{z}, 1]$ , where  $\bar{s} = 1$ . The difference increases when the size of the second portion ( $1 - \hat{z}$ ) related to the local OCAD approach increases. When the second portion disappears, the global OCAD approach reduces to the local OCAD approach. In addition, the value of  $\hat{z}$  decreases with  $Da$  for the local OCAD approach, while for the global OCAD approach it decreases slightly to a minimum value and then increases. Moreover, it

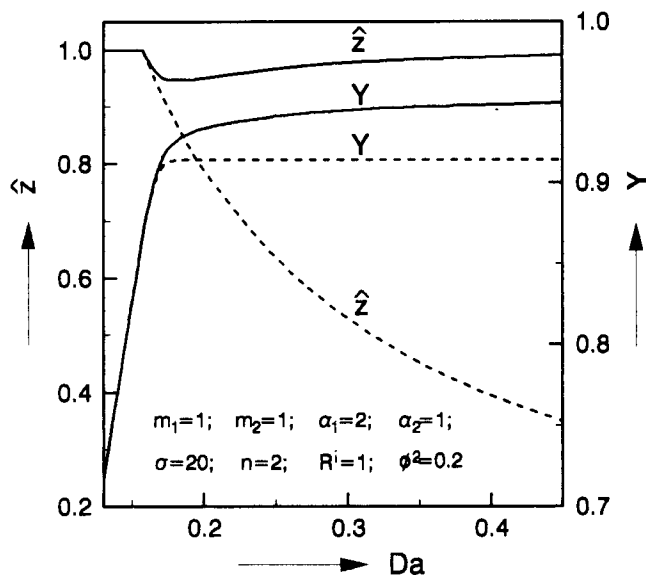


**Figure 3. Maximum outlet yields vs. values of  $\hat{z}$  from local OCAD approach (---) and global OCAD approach (—) as functions of the Damköhler number.**

can be expected that, as  $Da \rightarrow \infty$ ,  $\hat{z} \rightarrow 0$  for the former and  $\hat{z} \rightarrow 1$  for the latter, further indicating that through the global OCAD approach the whole reactor has been better utilized. For the global OCAD approach the increase of  $\hat{z}$  with  $Da$  at high values of  $Da$  is due to the dominant effect of the selectivity on the yield. Actually, when the value of  $Da$  is very high, the conversion is no longer a problem, and to get the maximum outlet yield one should consider how to improve the selectivity.

### Maximum outlet selectivity

In the following, we consider the case:  $m_1 = 2$ ,  $m_2 = 1$ ,  $\alpha_1 = 2$ , and  $\alpha_2 = 0$  in Eqs. 1 and 2, and then, Eqs. 7 and 8 become:

$$F_1(\bar{u}_1) = (1 + \sigma)^2 \cdot \frac{\bar{u}_1^2}{(1 + \sigma \cdot \bar{u}_1)^2} \quad (18)$$

$$F_2(\bar{u}_1) = \bar{u}_1 \quad (19)$$

It can be shown from Eq. 13 that in this case the local selectivity is maximized at  $\bar{u}_1 = 1/\sigma$ .

The two optimization approaches used for the maximum outlet yield are now used for the maximum outlet selectivity. The solutions based on the local OCAD approach and the global OCAD one are shown respectively in Figures 4 and 5, where  $\sigma = 10$ . Again, the global OCAD approach gives a higher outlet selectivity (for the chosen reacting system, the difference in the outlet selectivity from the two approaches is not very significant. Although the difference does exist, it is not due to the computational error).

Comparing the two profiles of  $S_c$  in Figures 4 and 5, one can find that the local selectivity in the case of Figure 4 is higher in the first portion of the reactor where the active location is below the external surface and it becomes inferior only in the second portion where the active location is at the

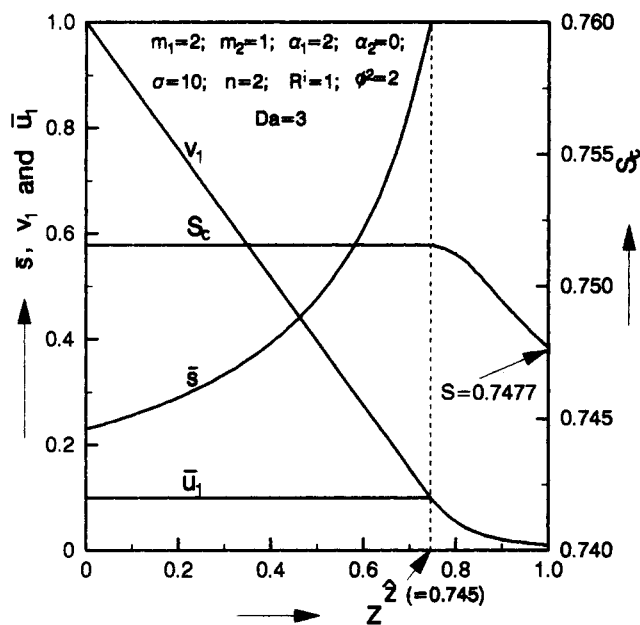


**Figure 4. Optimal solution for the maximum outlet selectivity from local OCAD approach.**

Profiles of the active location  $\bar{s}$ , the reactant concentration  $\bar{u}_1$  at  $s=\bar{s}$  and  $v_1$  in the fluid phase, and the local selectivity  $S_c$  along the reactor axis.

external surface. It implies that the second reaction is dominant in the second portion, leading to the decrease of the selectivity. In the case of Figure 5, the selectivity is slightly lower in the first portion, however, the size of the second portion has been reduced. The profit from the reduction of the second portion compensates well for the loss in the selectivity in the first portion, thus, giving rise to the higher outlet selectivity.

Finally, it should be pointed out that although the present study indicates that the global OCAD approach is superior to the local OCAD approach in some specific cases, whether the solution based on the global OCAD solution is the upper bound one for the problem under examination needs to be verified. Such verification has not been provided in this report. However, it is clear from the above observation that, indeed, the solution based on the local OCAD approach cannot be generally considered as the upper bound one, at least for the outlet yield and the outlet selectivity.

## Notation

- $a(s)$  = activity distribution function in pellets  
 $C$  = concentration  
 $D = D_{eA}/D_{eB}$   
 $Da$  = Damköhler number,  $\bar{k}_1 f_1(C_{Af}^i)(1-\epsilon)S_T/Q_T C_{Af}^i$   
 $D_e$  = effective diffusivity  
 $f$  = concentration-dependent portion in reaction rate expression, defined by Eq. 1 or 2  
 $F_i = (i=1,2)$  functions defined by Eqs. 7 and 8  
 $\bar{k}$  = volume-average reaction rate constant  
 $K$  = adsorption equilibrium constant  
 $l$  = axial coordinate along the reactor  
 $L$  = reactor length  
 $m_i = (i=1,2)$  kinetic parameters defined by Eqs. 1 and 2  
 $n$  = integer characteristic of pellet geometry: slab ( $n=0$ ), cylinder ( $n=1$ ), sphere ( $n=2$ )  
 $Q_T$  = total flow rate of the feed stream

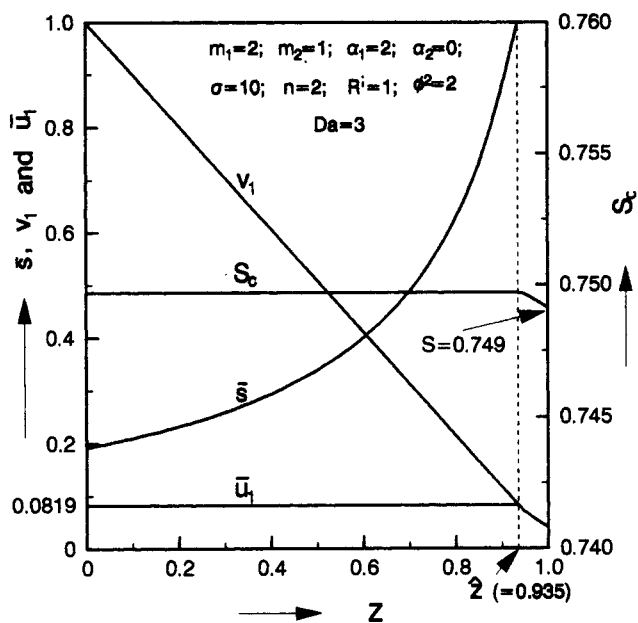


**Figure 5. Optimal solution for the maximum outlet selectivity from global OCAD approach.**

Profiles of the active location  $\bar{s}$ , the reactant concentration  $\bar{u}_1$ , at  $s=\bar{s}$  and  $v_1$  in the fluid phase, and the local selectivity  $S_c$  along the reactor axis.

- $r$  = distance from the center of the pellet; reaction rate  
 $R$  = function defined by Eq. 4 or 5  
 $R_p$  = characteristic pellet dimension: half-thickness ( $n=0$ ), radius ( $n=1,2$ )  
 $R^i = \bar{k}_2 f_2(C_{Af}^i)/\bar{k}_1 f_1(C_{Af}^i)$   
 $s = r/R_p$   
 $\bar{s}$  = dimensionless location of the catalyst activity in the pellet  
 $S_T$  = intersection area of the reactor  
 $u_i = (i=1)C_A/C_{Af}^i; (i=2)C_B/C_{Af}^i$   
 $\bar{u}_1 = u_1(\bar{s})$   
 $v_i = (i=1)C_A/C_{Af}^i; (i=2)C_B/C_{Af}^i$   
 $z = l/L$   
 $\hat{z}$  = value of  $z$  which indicates the portion of the reactor,  $z \in [0, \hat{z}]$  where the active location in pellets is below the external surface

## Greek letters

- $\alpha_i = (i=1,2)$  kinetic parameters defined by Eqs. 1 and 2  
 $\delta$  = Dirac delta function  
 $\epsilon$  = bed void fraction  
 $\sigma$  = kinetic parameter,  $K C_{Af}$   
 $\phi^2$  = Thiele modulus,  $R_p^2 \bar{k}_1 f_1(C_{Af}^i)/D_{eA} C_{Af}^i$

## Superscripts

- $i$  = value at the reactor inlet  
 $o$  = value at the reactor outlet

## Subscripts

- 1 = reactant A; reaction 1  
 2 = product B; reaction 2  
 $f$  = value in the fluid phase

## Literature Cited

- Dougherty, R. C., and X. E. Verykios, "Nonuniformly Activated Catalysts," *Catal. Rev. Sci. Eng.*, **29**, 101 (1987).

Gavrilidis, A., A. Varma, and M. Morbidelli, "Optimal Distribution of Catalyst in Pellets," *Catal. Rev. Sci. Eng.*, **35**, 399 (1993).  
Morbidelli, M., A. Servida, S. Carrà, and A. Varma, "Optimal Catalyst Activity Profiles in Pellets: 5. Optimization of the Isothermal Fixed-Bed Reactor," *Ind. Eng. Chem. Fundam.*, **25**, 313 (1986a).  
Morbidelli, M., A. Servida, and A. Varma, "Optimal Catalyst Activity Profiles in Pellets; 4. Analytical Evaluation of the Isothermal Fixed-Bed Reactor," *Ind. Eng. Chem. Fundam.*, **25**, 307 (1986b).  
Morbidelli, M., A. Servida, and A. Varma, "Optimal Catalyst Activity

Profiles: 1. The Case of Negligible External Mass Transfer Resistance," *Ind. Eng. Chem. Fundam.*, **21**, 278 (1982).  
Wu, H., A. Brunovska, M. Morbidelli, and A. Varma, "Optimal Catalyst Activity Profiles in Pellets: VIII. General Nonisothermal Reacting Systems with Arbitrary Kinetics," *Chem. Eng. Sci.*, **45**, 1855 (1990).

Manuscript received Aug. 5, 1993, and revision received Oct. 25, 1993.

**Statement of Ownership, Management, and Circulation** required by 39 U.S.C. 3685 of October 10, 1994, for the *AIChE Journal*, Publication No. 002-580, issued monthly for an annual subscription price of \$445.00 from 345 E. 47th St., New York, NY 10017, which is the location of its publication and business offices. The names and addresses of the Publications Director and Editors are: Managing Director, Publications, Stephen R. Smith, 345 E. 47th St., New York, NY 10017; Editor, Dr. Matthew V. Tirrell, Department of Chemical Engineering and Materials Science, University of Minnesota, Minneapolis, MN 55455; and Managing Editor, Haeja L. Han, 345 E. 47th St., New York, NY 10017. The owner is: American Institute of Chemical Engineers, 345 E. 47th St., New York, NY 10017. The known bondholders, mortgagees, and other security holders owning or holding 1% or more of the total amounts of bonds, mortgages, or other securities are: none. The purpose, function, and nonprofit status of this organization and the exempt status for federal income tax purposes have not changed during the preceding 12 months. The following figures describe the nature and extent of *AIChE Journal* circulation. In each category the first number (*in italics*) is the *average number of copies of each issue during the preceding 12 months*. The number next to it, within parentheses ( ), is the actual number of copies of the single issue published nearest to the filing date. Total number of copies printed (net press run), *3,916* (4,000). Paid circulation: 1. sales through dealers and carriers, street vendors, and counter sales, none; 2. mail subscriptions, *2,806* (2,817). Total paid circulation *2,806* (2,817). Free distribution, by mail, carrier, or other means, of samples, complementary, and other free copies: *49* (46). Total distribution: *2,855* (2,863). Copies not distributed: 1. office use, leftover, unaccounted, spoiled after printing, *1,061* (1,137). 2. returns from news agents, none. Total: *3,916* (4,000). I certify that the statements made by me are correct and complete. Managing Director, Publications, Stephen R. Smith.